

See discussions, stats, and author profiles for this publication at: <https://www.researchgate.net/publication/281119460>

Optically Transparent Carbon Nanotube Film Electrode for Thin Layer Spectroelectrochemistry

ARTICLE in ANALYTICAL CHEMISTRY · AUGUST 2015

Impact Factor: 5.64 · DOI: 10.1021/acs.analchem.5b01784

READS

10

5 AUTHORS, INCLUDING:



Tingting Wang

University of Texas at Austin

14 PUBLICATIONS 61 CITATIONS

[SEE PROFILE](#)



Vesselin Shanov

University of Cincinnati

152 PUBLICATIONS 1,962 CITATIONS

[SEE PROFILE](#)

Optically Transparent Carbon Nanotube Film Electrode for Thin Layer Spectroelectrochemistry

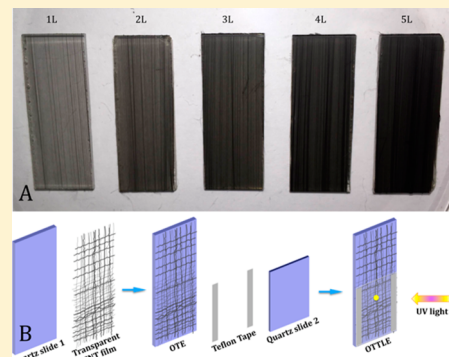
Tingting Wang,[†] Daoli Zhao,[†] Noe Alvarez,[‡] Vesselin N. Shanov,[‡] and William R. Heineman*,[†]

[†]Department of Chemistry, University of Cincinnati, Cincinnati, Ohio 45221-0172, United States

[‡]Department of Biomedical, Chemical and Environmental Engineering, University of Cincinnati, Cincinnati, Ohio 45221-0012, United States

Supporting Information

ABSTRACT: Carbon nanotube (CNT) film was evaluated as an optically transparent electrode (OTE) for thin layer spectroelectrochemistry. Chemically inert CNT arrays were synthesized by chemical vapor deposition (CVD) using thin films of Fe and Co as catalysts. Vertically aligned CNT arrays were drawn onto a quartz slide to form CNT films that constituted the OTE. Adequate conductivity and transparency make this material a good OTE for spectroelectrochemistry. These properties could be varied by the number of layers of CNTs used to form the OTE. Detection in the UV/near UV region down to 200 nm can be achieved using these transparent CNT films on quartz. The OTE was characterized by transmission electron microscopy, scanning electron microscopy, Raman spectroscopy, UV-visible spectroscopy, cyclic voltammetry, electrochemical impedance spectroscopy, and thin layer spectroelectrochemistry. Ferricyanide, tris(2,2'-bipyridine) ruthenium(II) chloride, and cytochrome c were used as representative redox probes for thin layer spectroelectrochemistry using the CNT film OTE, and the results correlated well with their known properties. Direct electron transfer of cytochrome c was achieved on the CNT film electrode.



Spectroelectrochemistry is the combination of species-focused spectroscopy with reaction-oriented electrochemistry.¹ It enables simultaneous spectral observation through the electrode with electrochemical control.² Typical spectroscopic methods in spectroelectrochemistry include UV-visible absorption and fluorescence, near-infrared and infrared absorption, Raman spectroscopy, and electron paramagnetic resonance.¹ Spectroelectrochemical cells require optical transparency for cell material, electrolyte, and the electrode itself for those techniques in which light is passed through the electrode.¹ Currently, transparent electrode materials such as grids or thin films of Au, Pt, indium tin oxide (ITO), and carbon and fiber optics that allow the transmission of the changes occurring at or adjacent to the electrode surface are commonly used.^{3–6} A narrow thickness of the electrolyte layer contacting the working electrode shortens the time for complete electrolysis in the optically transparent thin layer electrode (OTTLE).^{5–7} The spectroelectrochemical properties of the redox species being characterized (analyte) are then monitored by controlling the applied potential.¹ Spectroelectrochemistry in the UV and IR regions is often limited by the absorption of electrolyte and electrode material itself.¹ Candidates for spectroscopically transparent materials are sought for spectroelectrochemistry in those regions.

The development of carbon optically transparent electrodes (OTEs) has been a longstanding interest in the spectroelectrochemistry field because of carbon's unique characteristics. The first carbon OTE consisted of a thin carbon film (15–31

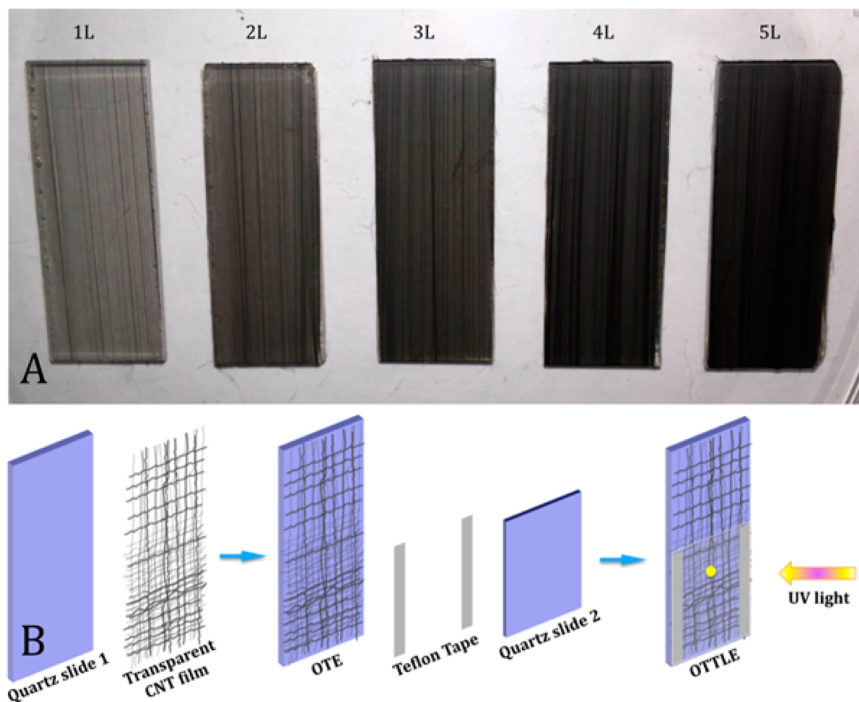
nm) vapor-deposited on a heated quartz or glass substrate.⁸ Electrode properties similar to those of conventional graphite electrodes were obtained with a higher resistance of 1000–1700 Ω/\square .⁸ Later, carbon OTEs with substantially improved conductivity were prepared by vapor depositing carbon on ITO OTEs to obtain the electrode properties of carbon but with improved conductivity provided by the overcoated ITO layer.⁹ Reticulated vitreous carbon (RVC), a foam material, was first used as an OTE for thin-layer spectroelectrochemical studies in molten salts where ruggedness to high temperature is important.¹⁰ RVC also proved useful for extended X-ray absorption fine structure thin-layer spectroelectrochemistry where the transparency of carbon to X-rays is important.¹¹ The advent of carbon nanotube (CNT) materials stimulated the development of carbon OTEs consisting of thin films of CNTs to take advantage of the unique properties of their transparency and conductivity. However, fabricating and constructing CNT OTEs with proper resistance and good light transmission also challenges their wider application.¹²

With the emergence of nanoscale materials, intense research has driven the exploration of optical, electrical, and mechanical properties of nanostructured materials such as carbon, metal grids, and metallic wires.¹³ The thickness of nanostructured films is ultrathin, typically 1–100 nm, which enables excellent

Received: May 12, 2015

Accepted: August 20, 2015

Scheme 1. (A) Photographs of OTEs with 1 to 5 Layers of Parallel-Assembled CNT Films on Quartz; (B) Assembly of the CNT Film OTE and OTTLE



transparency.¹² Among all the nanoscale materials, CNTs have become the most widely studied since their discovery.¹⁴ Their unique structural, chemical, and electronic properties as well as their chemical stability have led to useful commercial applications from batteries and chemical sensors to water filters and sporting goods.^{15–17} Chemical vapor deposition (CVD) is the dominant technique currently used for bulk fabrication of CNTs.¹⁸ In CVD, hydrocarbon precursors (e.g., methylene, ethylene, acetylene) are irreversibly decomposed at a temperature of 600–1200 °C depending on the choice of precursors, and as hydrogen is carried away and carbon precipitates, CNTs start growing from either the top or base of the catalyst.^{19–21} Understanding the CVD process enables the synthesis of CNTs with desired properties and forms. The diameter, length, and purity level of powders, yarns, forests, threads, and films relate closely to the choice of precursors, catalysts, and process conditions.^{22–29}

Widespread developments and assessments of CNT transparent films have demonstrated the great potential of this material in many commercial applications.¹⁵ Wu et al. first reported fabrication and application of transparent single-walled carbon nanotubes (t-SWNTs) to construct an electric field-activated optical modulator.³⁰ Chen et al. illustrated the mass production of CNT films from drawing the sidewall of a multiwalled carbon nanotubes (MWCNTs) forest and developed a super capacitor based on this material.³¹ Cai et al. developed a multifunctional capacitive strain sensor to detect strains up to 300% based on superstretchable and transparent CNT films.³² Many other applications of CNT films can be found in recent reports.^{33–37}

As the exploration of transparent conducting CNT films continues, spectroelectrochemistry and spectroelectrochemical sensors are becoming increasingly important and feasible applications for this material. Herein, we report an OTE made from a multiwalled CNT vertically aligned film and

demonstrate for the first time its application for visible wavelength spectroelectrochemistry. The constructed CNT film-based OTE showed good transparency in the UV region. This OTE shows special promise for use in thin layer spectroelectrochemistry with an OTTLE where transparency into the UV and the electron transfer characteristics of a carbon-based electrode are important. The OTE properties were characterized by transmission electron microscopy (TEM), scanning electron microscopy (SEM), UV–visible absorption spectroscopy, cyclic voltammetry, and electrochemical impedance spectroscopy. Tris(2,2'-bipyridine) ruthenium(II) chloride was used as a representative redox system to demonstrate the utility of the CNT OTE for thin layer spectroelectrochemistry. Application to cytochrome c as a representative biological redox protein showed direct oxidation/reduction at the CNT film OTTLE.

■ EXPERIMENTAL SECTION

Reagents. Drawable CNTs were synthesized by a CVD process that has been published elsewhere.^{38,39} Briefly, synthesis starts with catalyst deposition; thin films of Fe and Co were used as catalyst (1.2 nm). They were sputtered on 4 in. Si wafers that had a 5 nm Al₂O₃ buffer layer, also deposited by sputtering. The Si wafer substrates were scribed and broken into 2 in. long and variable width (up to 1.5 in.) substrates that were loaded into a commercial CVD reactor (ET3000 from CVD Equipment Corporation). The growth process took place at 740 Torr pressure. The reactor was heated to 400 °C for annealing under Ar; after 2 min, the reactor was ramped to 750 °C, and a mixture of 300 sccm C₂H₄ and 1000 sccm Ar was introduced at this temperature for 20 min. Upon growth completion, 30 sccm of H₂O and 2000 sccm of Ar were delivered during cooling to promote CNT array detachment. Detached CNT arrays were transferred onto a Si wafer or other flat substance such as glass, quartz, etc. Transparent CNT

ribbon drawing starts at one edge of the CNT array and continues until the CNT array is consumed at the opposite edge. During this process, no other chemical or binder is required to assemble individual CNTs into films and threads. van der Waals forces between CNTs allows the ribbon assembly process. Approximately each millimeter of CNT array allows one to draw a meter of ribbon.^{28,40} Cytochrome c from equine heart ($\geq 95\%$) and all the other chemicals were purchased from Sigma-Aldrich Inc. and used without further purification. Deionized water was used for preparing all solutions (Nanopure water purification system).

Instrumentation. TEM images of the CNTs were taken with a FEI Tecnai F20 S/TEM using a 200 kV beam. SEM micrographs were obtained using an environmental scanning electron microscope ESEM Philips XL-30 Field Emission at an acceleration voltage of 15 kV and 15 mm work distance. Raman spectra were acquired with a Renishaw In Via micro Raman spectrometer, 514 nm wavelength. EIS was performed with a Gamry Reference 600 (Gamry Inc.). The dc potential was set at 0 mV vs open circuit potential (OCP) with a perturbation potential of 5 mV. The frequency range was from 10^5 to 0.1 Hz. Cyclic voltammetry was performed with a BASi 100B Electrochemical Analyzer (BASi). In cyclic voltammetry, an initial negative scan was conducted, unless otherwise stated. A CNT film coated quartz slide was used as the working electrode unless a CNT film coated glassy carbon (GC) is stated as the working electrode. A 10 mL small beaker was equipped with a Ag/AgCl (3 M KCl) reference electrode or Pt quasi-reference electrode and a Pt wire auxiliary electrode for characterizing CNT films by CV. This was replaced by a Pt wire quasi-reference electrode for EIS experiments.

OTE and OTTLE Preparation. OTEs were constructed using quartz slides (40 mm \times 10 mm \times 1 mm) custom-made by Chemglass Life Sciences. Prior to use, each quartz slide was thoroughly rinsed with ethanol and H₂O, followed by drying with compressed air. Each CNT film electrode was made by directly drawing from CNT arrays using either tweezers or an automatic drawing device and applying the array as a film on a quartz slide as shown in **Scheme 1**. A single layer of aligned CNT film employed in this work is typically 40 nm thick. The absorption/transmission properties of this material were characterized using the as-made dry OTE. For CV and EIS experiments, the OTEs were directly connected with an alligator clip to the potentiostat in a conventional electrochemical cell and only part of the OTE (25 mm \times 10 mm) was in contact with the solution. When making OTTLEs, 1–2 layers of CNT films were placed on the quartz slide where the light would pass through and more layers of CNT films were aligned on the rest of the quartz to increase the conductivity of the electrode. Another quartz slide (25 mm \times 10 mm \times 1 mm) was then positioned on the CNT film OTE to form the OTTLE (**Scheme 1B**). The two slides were separated by a pair of silicone spacers with a thickness of ~ 0.18 mm. The cell was then glued with epoxy (Loctite-model # 1395391, purchased from Home Depot) along the side and top edges (leaving an opening in the top), and the epoxy was cured in air. A specially designed holder was used for spectroelectrochemistry.⁴¹ Solution added to the container was drawn into the OTTLE by vacuum aspiration through the opening in the top. The electrochemical cell was completed with a miniature Ag/AgCl, 3 M KCl reference electrode (EDAQ Inc. ET073) and a Pt wire auxiliary electrode that were dipped into the solution in the holder.

RESULTS AND DISCUSSION

Microscopy and Spectroscopy. Basic properties of the CNT films such as structure, composition, quality, and transparency are important for determining the application of this material. Structural characteristics of the CNT film were obtained with TEM and SEM. TEM showed that a multiwalled nanotube structure was clearly present in these CNT materials. The CNTs are about 400 nm in length and 10 nm in width (**Figure 1A,B**). The SEM images of a single layer of CNT film

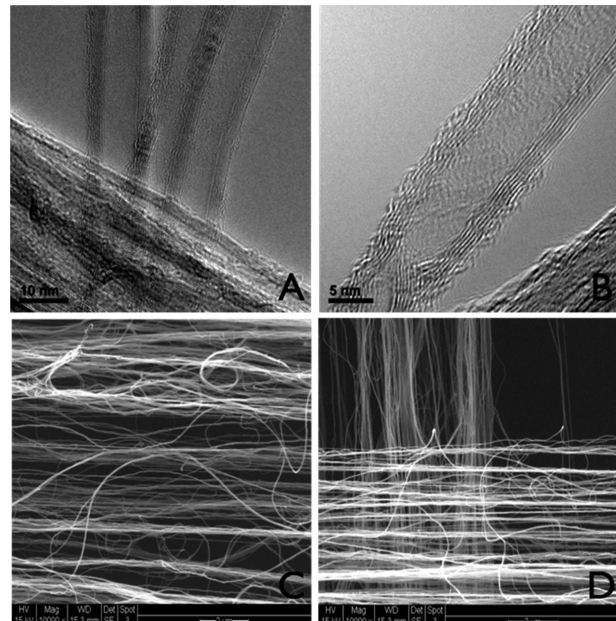


Figure 1. TEM images of the as synthesized CNT material at (A) lower and (B) higher magnifications. SEM images of (C) a single layer of CNT film and (D) a cross-assembled double layer CNT film.

displayed a generally parallel alignment of the nanotube threads with some threads randomly oriented. Optical transparency of the films is due to the spaces between the threads and the thinness of the threads themselves (**Figure 1C**). Multiple layers of CNT film could be assembled by stacking the films in either a parallel orientation or a perpendicular (cross) orientation. A SEM image of two layers of cross-assembled CNT films is shown in **Figure 1D**. Both orientations were initially explored and gave similar results. The parallel orientation was used for the work reported here because the OTEs were easier to make.

Raman spectroscopy has become especially useful for studying CNTs. The diameter of the nanotubes, the nanotube interactions, and the disorder present in the sp² hybridized carbon system can be assessed by Raman spectroscopy.⁴² Three typical graphite bands were found with the CNT film: (1) the G band at ~ 1594 cm⁻¹ is the characteristic feature of carbon atom vibration; (2) the G' band at ~ 2708 cm⁻¹ is observable for defect free sp² carbons; and (3) the D band represents the defective graphite structure (~ 1362 cm⁻¹). The ratio of the D band to G band measures the quality of the material: the higher the ratio, the more defects exist in the material. In this case, the D/G ratio of CNT film is relatively lower than the CNT disk we studied before, indicating a lower quantity of structural defects (**Figure 2**).

Optical images of OTEs were taken with layers of parallel-assembled CNT films from 1 to 5 layers on quartz. As expected,

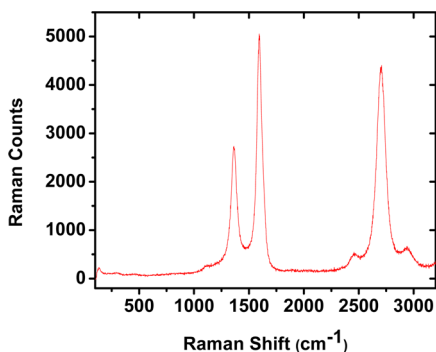


Figure 2. Raman spectrum of CNT film.

the transparency visible to the eye decreased with increasing number of CNT layers ([Scheme 1A](#)).

UV-visible absorption spectra of as-made dry OTEs with 1–5 layers of CNT film on quartz are shown in [Figure 3](#). The characteristic band at 200–300 nm in the absorption spectrum for a simple graphene layer is known as the π plasma resonance; it originates from the peak (energy of the absorbance) in the joint density of states.⁴³ For CNTs, this peak can shift and split due to the more complex band structure.^{44,45} These spectra confirm that the transparency of the CNT film is a combination of light passing between as well as through the individual fibers. Furthermore, by using the CNT transparent film, the detectable wavelength region in a UV-vis spectrometer can be extended to as low as 200 nm, which is comparable to a 100 line per inch gold mesh OTE and 100–150 nm deeper in the UV compared to commercial ITO transparent electrodes ([Figure S1](#)). The comparison with customized ITO (135 nm thick coated on glass) and gold mesh shown in [Figure S1](#) confirms that CNT film is transparent in the UV region at 1–2 layers, that ITO is more transparent in the visible region, and that gold mesh is the most transparent in the UV region. The absorption spectra also showed that more layers of CNT film gave a linear increase in absorbance at 250 and 600 nm with 1–5 CNT film layers ([Figure 3](#), insets). Besides parallel-assembled CNT films, absorption spectra of cross-assembled CNT films were also taken and similar absorbance responses were obtained ([Figure S2](#)). Reproducibility of the transparency from electrode to

electrode was good within the same batch of CNT film. For example, a single layer of CNT film gave a standard error of 0.66 %T for three replicates from the same batch at 250 nm, whereas the error increased to 1.3 %T when the three electrodes were made from different batches.

Cyclic Voltammetry. The electrochemical behavior of the parallel-assembled CNT films was investigated by cyclic voltammetry (CV). In these and subsequent experiments, the OTE was immersed in a bulk solution of aqueous electrolyte, and the CNT films were found to adhere very well to the underlying quartz, except the single layer hydrophobic CNT films tended to aggregate immediately after contact with the supporting electrolyte ([Figure S3](#)), while with more than two layers of CNT film less aggregation was observed. However, no problems with detachment of the CNT films from the quartz were experienced. CVs of the CNT film OTE were essentially featureless over a wide potential range. The comparison of a CNT film OTE with commercial ITO and Au electrodes (surface areas were normalized) in 0.1 M KCl supporting electrolyte ([Figure 4A](#)) shows essentially flat voltammograms for the CNT film OTE and ITO that are indistinguishable on this current scale, whereas the CV for gold is dominated by the large peak in the positive potential region, which is consistent with oxidation in chloride forming AuCl_4^- .⁴⁷

Expansion of the current axis (inset) shows the CNT OTE to have a wider potential range, especially at the negative potential limit, than ITO. The CNT film was the most inert in 0.1 M KCl supporting electrolyte ([Figure 4A](#), inset, red trace), having no prominent peaks as for Au ([Figure 4A](#), black trace that goes off-scale). A further comparison of different layers of CNT films in supporting electrolyte was performed. As expected, the capacitance current increased with increasing layers of CNT film ([Figure 4B](#)). The enhancement of current is attributed to the increase in the active surface area of the CNT films on the quartz slide, as other parameters such as the area of the quartz/CNT film immersed in the solution, electrolyte concentration, scan rate, etc. were kept the same.

From the CVs in [Figure 4B](#), the capacitances of the CNT films can be calculated using a previously reported method, and they were found to increase linearly as 37, 81, 138, 186, and 233 $\mu\text{F}/\text{cm}^2$ for 1 to 5 layers of CNT films, respectively.⁹ Similar capacitances were found with cross-assembled CNT films. One

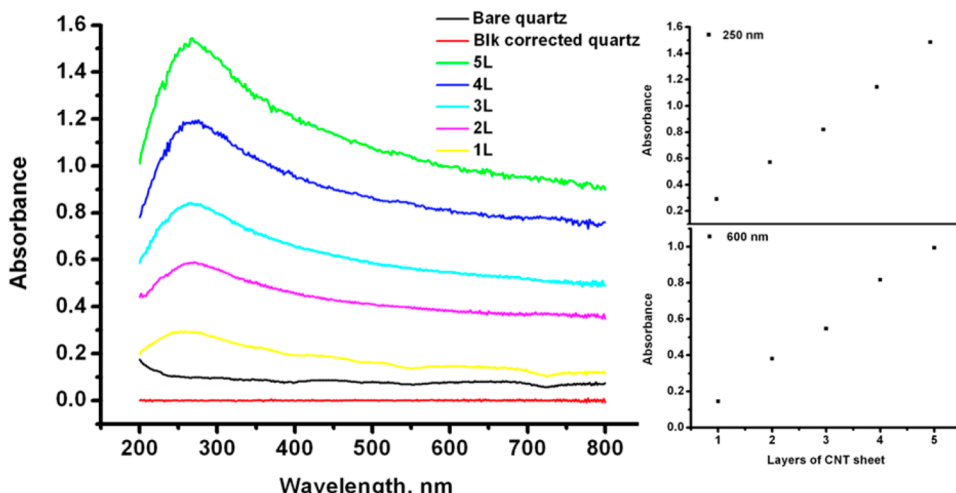


Figure 3. Absorption spectra of 1–5 layers of CNT film on a quartz slide. The absorbance of quartz (black line) was subtracted when acquiring the absorbance of the CNT films. Inset: Absorbance vs layers of CNT at 250 and 600 nm. Parallel-assembled CNT films were used.

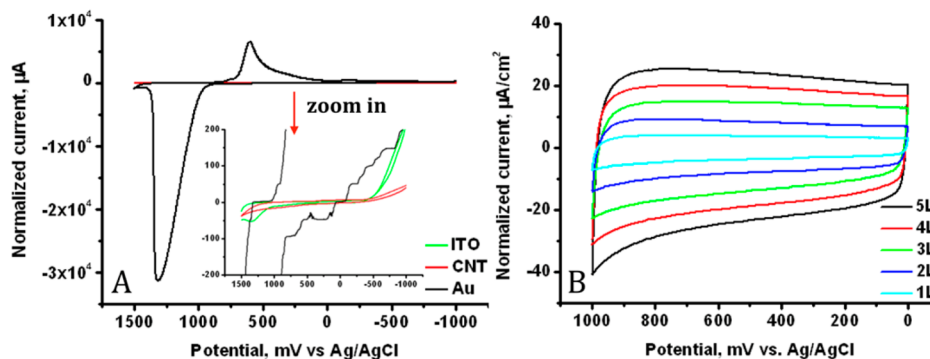


Figure 4. (A) Cyclic voltammetry comparison of 1 layer CNT film with ITO and Au in 0.1 M KCl. (B) Cyclic voltammetry of 1–5 layers of parallel-assembled CNT films on quartz slide in 1 M Na₂SO₄. Scan rate was 100 mV/s. Scans initiated at OCP in the negative direction. Parallel-assembled CNT films were used.

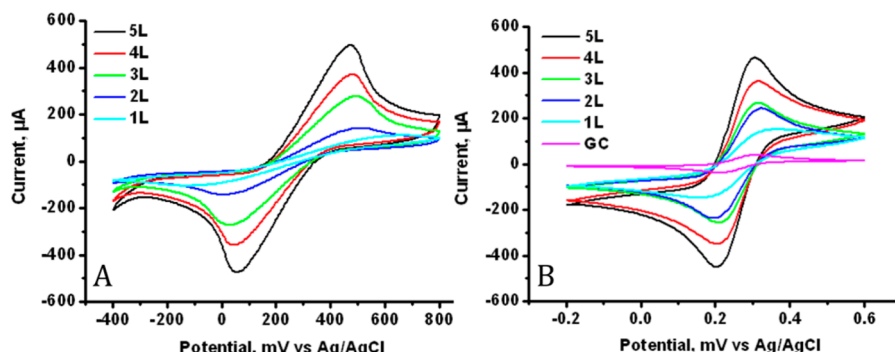


Figure 5. Cyclic voltammetry of 1–5 layers of CNT films on (A) quartz and (B) GC electrode. Two mM K₃Fe(CN)₆ in 1 M KCl. Scan rate: 100 mV/s. Parallel-assembled CNT films were used.

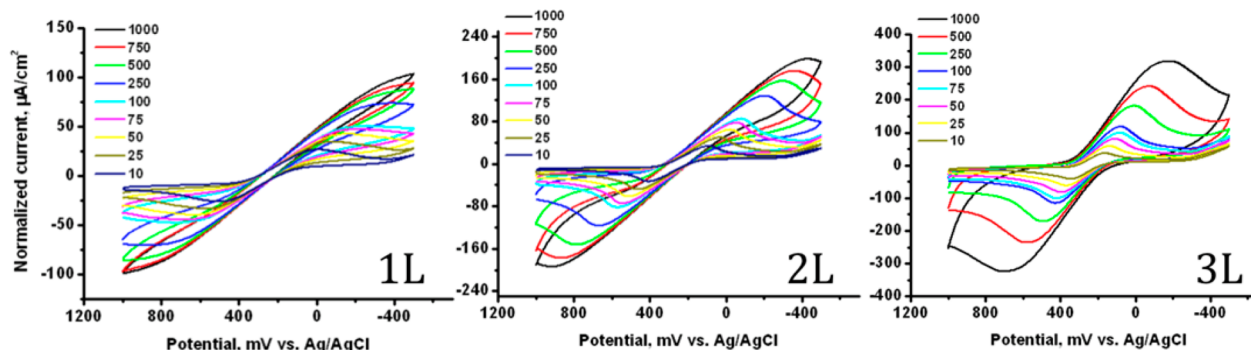


Figure 6. Representative scan rate studies of 1–3 layers of CNT films on quartz. 2 mM K₃Fe(CN)₆ in 1 M KCl was used as the analyte and supporting electrolyte. Scan rate was varied from 10 to 1000 mV/s. Parallel-assembled CNT films were used.

interesting phenomenon was observed when 10 layers of CNT film were used: no significant differences in capacitive currents were found compared with 40 layers (data not shown). This is probably due to the hydrophobicity of the CNT film, causing poor contact of the electrolyte with the inner layers of CNT film near the quartz.

Ferricyanide was used as a representative redox probe to examine electrochemical performance of the CNT film OTE with respect to electrode resistance and electron transfer properties. When ferricyanide was added, the anodic and cathodic peak currents with respect to the CNT films layers were observed (Figure 5A, Table S1). The CVs obtained in a bulk solution of ferricyanide were well-defined as shown in Figure 5A, while the peak separations were much larger than the theoretical value of 59 mV for a one-electron transfer for

ferri/ferrocyanide (Table S1). At the same scan rate, the peak separation for 5 layers of CNT films is about 400 mV smaller than for 1 layer of CNT film, but it is still much larger than the theoretical peak separation of 59 mV (Figure 5A). The fact that peak separation decreases with increasing peak current as the number of CNT films increases suggests that the large peak separation is due to electrode resistance of the CNT film rather than slow electron transfer with ferri/ferrocyanide. This point was examined in more detail with further studies in which CNT films were applied on a commercial glassy carbon (GC) electrode where the underlying GC serves as a current transducer to the overlaid CNT film, yet it does not expose surface to the solution and so does not contribute measurably to the electron transfer with ferri/ferrocyanide. This CNT film covered GC electrode exhibits much more reversible CVs as

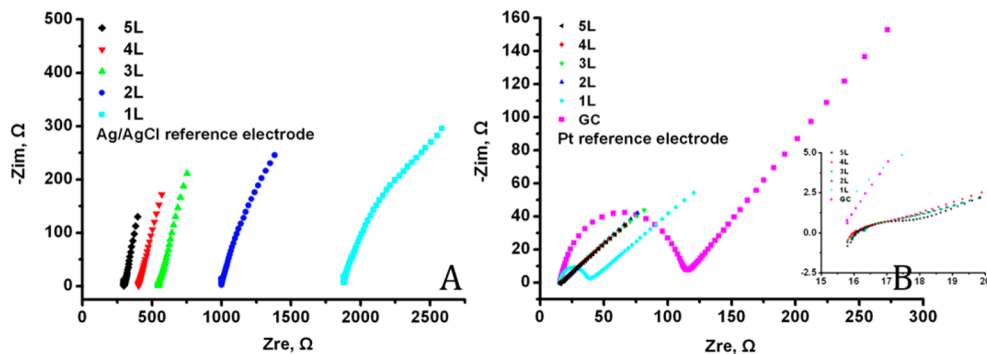


Figure 7. (A) EIS of 1–5 layers of CNT films on quartz. Ag/AgCl (3 M KCl) was used as the reference electrode. (B) EIS of GC and 1–5 layers of CNT films modified GC electrodes. Pt wire was used as the reference electrode. 5 mM of equal concentrations of $K_3Fe(CN)_6/K_4Fe(CN)_6$ in 1 M KCl was the analyte and supporting electrolyte. Inset: zoom in of the higher frequency range of the impedance. Parallel-assembled CNT films were used. OCP was applied.

shown in Figure 5B. Two layers of CNT film-modified GC electrode give a peak separation of only 100 mV compared to 485 mV on quartz. The dramatic peak separation improvement is attributed to the much lower resistance of the GC as a current transducer that makes contact with the entire CNT film from its back side, reducing the CNT resistance to the thickness of the CNT film(s). By comparison, the CNT films on quartz are connected at only one edge, making the resistance a gradient along the entire length of the film, which is significantly greater. When only 1 and 2 layers of CNT films were applied, the CVs were a combination effect from both GC and CNT film, since the contact between solution and GC was visibly identified, and the CNT film-modified GC electrode had higher current than the CNT film alone. However, when more than 2 layers of CNT film were applied, no direct contact between the analyte and GC electrode surface was observed; therefore, the contribution of electrochemistry at the GC electrode to the cyclic voltammogram can be neglected. Currents shown in Figure 5 were not normalized with the surface area because the surface area varied from the combination of GC and CNT film to CNT film alone, and the real surface area from the combination behavior is difficult to determine.

The resistance of the CNT film was determined using Ohm's law in conjunction with a scan rate study for different layers of CNT film on quartz shown in Figure 6. The increase in peak separation is evident as the scan rate increases, caused by increasing IR drop as a result of current enhancement. However, the magnitude of the peak separation is decreased with increasing layers of CNT films. The slopes obtained from the linear regression of peak potentials versus peak currents correspond to the combined resistances of the CNT film and the solution. For 1–3 layers of CNT films, the resistances were determined to be 1700 ± 400 , 1400 ± 700 , and $450 \pm 40 \Omega$, respectively. Thus, from a strictly electrochemical point of view, it is better to use multiple layers of CNT films to reduce IR drop of the OTE.

Electrochemical Impedance Spectroscopy. Besides CV, electrochemical impedance spectroscopy (EIS) is another effective technique for studying the resistance of an electrode material. It can provide information about the interfacial properties of an electrode surface, such as electrode/solution resistance (R_s), heterogeneous charge transfer resistance (R_{ct}) at the interface, and double layer structure (C_{dl}).⁹ EIS was initially carried out with 1–5 layers of CNT film on quartz

slides. A high electrode/solution resistance was found for a single layer, and as layers of CNT films increased, the R_s dropped, which was due to the increasing conductivity of more layers of CNT films (Figure 7A). The R_s obtained from the Nyquist plot was in agreement with the measured resistances in the scan rate study: 1871Ω (1L), 997Ω (2L), 543Ω (3L), 403Ω (4L), and 297Ω (5L). However, little kinetic information can be extracted because the system was dominated by the high R_s , indicated by a lack of R_{ct} in the Nyquist plot (Figure 7A) caused by very fast heterogeneous electron transfer for the $Fe(CN)_6^{3-}/Fe(CN)_6^{4-}$ redox couple. In order to study the intrinsic charge transfer resistance, CNT films were then applied on a conductive GC electrode, as described above, and Pt wire was used as the reference electrode to further reduce the system resistance. Using this setup, the R_s of layers of CNT films was reduced to a few ohms as shown in Figure 7B. The R_{ct} of $Fe(CN)_6^{3-}/Fe(CN)_6^{4-}$ redox couple at the electrode interface was detected at this CNT modified GC electrode. Starting from 2 layers of CNT films, stretched out semicircles were obtained, which have typically been observed for porous structures of CNT film.⁴⁶ The R_{ct} of 2 and more layers of CNT films were found to be less than 1Ω , demonstrating the small intrinsic resistance of the CNT covering the GC electrode. The EIS results correlated well with the CV studies described above with 2–5 layers of CNT, where the peak to peak separations remained the same, suggesting similar kinetic properties with 2 and more layers of CNT films.

Thin Layer Spectroelectrochemistry. On the basis of the results of the spectroscopic and electrochemical studies discussed above, use of the CNT film OTE for spectroelectrochemistry requires consideration of both the transparency and the conductivity of the electrode since fewer CNT films gave better transparency but poorer conductivity. Also, as discussed in the CV and EIS experiments, fewer layers (1 or 2) of CNT films tend to aggregate after contact with aqueous supporting electrolyte, which enables excellent transparency of the OTE in the UV–visible region when light is passing through the spaces between the aggregated CNT films. However, fewer layers of CNT films were found to have higher resistance. Of the various types of spectroelectrochemical techniques, the CNT film OTE in the form shown in Scheme 1B seems most suitable for thin layer spectroelectrochemistry, which is least affected by electrode resistance. An electrode design consisting of 2 layers of parallel-assembled or cross-assembled CNT film was used in the lower region where

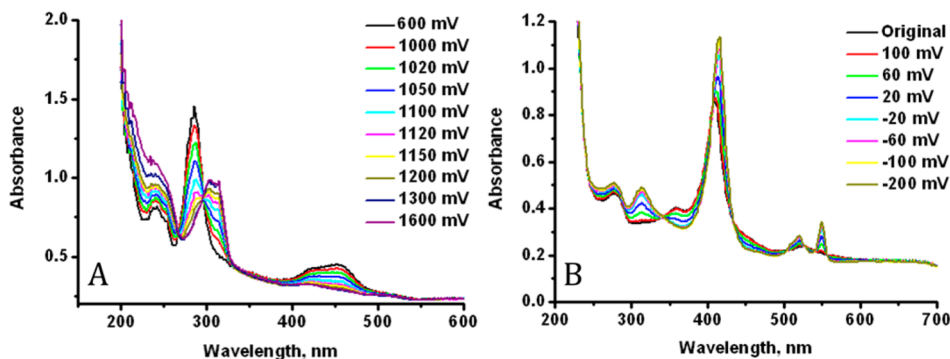


Figure 8. Absorption spectra of (A) 0.5 mM $\text{Ru}(\text{bpy})_3^{2+}$ in 1 M KCl and (B) 0.05 mM cytochrome c in 0.1 M, pH 7.2 PBS buffer with 1 M KCl. Constant potentials were applied as indicated in the figure. Equilibrium was determined when the current was stable, and the absorbance remained the same after three continuous recordings. Absorbances at 286 and 314 nm were used to calculate the n value and reduction potentials of $\text{Ru}(\text{bpy})_3^{2+}$ and cytochrome c, respectively.

the light beam would pass through, and more layers of cross-assembled CNT films were applied over the remainder of the quartz slide above and below the optical region to increase the conductivity of this section of the OTE whose only function is to carry current. This minimizes electrode resistance and maximizes transparency for spectroelectrochemistry experiments (**Scheme 1B**).

An OTTLE based on **Scheme 1B** was initially tested with $\text{Ru}(\text{bpy})_3\text{Cl}_2$ using the spectropotentiostatic approach to obtain spectra, reduction potential, and electron stoichiometry (n value).^{37,49} Figure 8A shows the absorption spectra of 0.5 mM $[\text{Ru}(\text{bpy})_3]^{2+}$ at a series of increasingly positive applied potentials that incrementally converted $\text{Ru}(\text{bpy})_3^{2+}$ to $\text{Ru}(\text{bpy})_3^{3+}$. Each potential was maintained until the solution redox couple equilibrated with the applied potential as evidenced by no further changes in the spectrum and a low current, which minimizes the effect of IR drop in the thin layer cell. Typically, absorption spectra were taken at 1 min intervals for each constant potential until the spectra became identical. On average, it took about 8 min for 0.5 mM $\text{Ru}(\text{bpy})_3^{2+}$ in the OTTLE to reach equilibrium with an applied potential. The absorption at 452 nm corresponds to the metal to ligand charge transfer, and the absorptions at 286 and 350 nm are associated with a $\pi^*-\pi$ transition and a d-d transition, respectively.⁴⁸ One of the advantages of using the CNT film OTE compared to ITO is that the usable wavelength range is extended below 300 to 200 nm, where in this case, the absorption at 286 nm was well distinguished from background compared with using a commercial ITO electrode which has a high absorbance at this wavelength. Using the thin layer spectroelectrochemistry version of the Nernst equation (absorbance at 286 nm was used for the calculations), the number of electrons transfer (n value) was measured as 0.85 ± 0.07 .^{37,49} The E°' determined by this method is 1099 ± 4 mV vs Ag/AgCl, which is close to the reported E°' of 1070 mV vs Ag/AgCl with 1 M KNO_3 as the supporting electrolyte.⁴¹ The somewhat low n value is attributed to the strong oxidizing property of the electro-generated $\text{Ru}(\text{bpy})_3^{3+}$ which makes it hard to maintain in the thin layer cell because of its chemical reactivity.

Horse heart cytochrome c is a relatively simple metalloprotein, which is often used to provide insight into the physiological electron transfer process for evaluation of a bioelectrocatalytical system.⁵⁰ Direct electrochemistry of cytochrome c at ITO electrode has been reported before, and it is mostly believed that the direct electrochemistry is achieved

by the adsorption of cytochrome c on ITO driven by electrostatic interaction between oppositely charged ITO electrode and cytochrome c. The adsorption time usually varies from several minutes to hours, and in order to omit the influence from unabsorbed cytochrome c, the electrochemical measurement is usually performed in a protein free condition.

In our study, complete electrolysis of solution soluble cytochrome c can be achieved using CNT film alone inside the OTTLE within several minutes.^{51–53} The immediate direct electron transfer between a CNT film and cytochrome c has been previously observed, and the mechanism attributed to the presence of MWCNTs changing the secondary structure of cytochrome c to expose the active site, where the spatial orientation of the heme is improved for direct electron transfer.⁵⁴ Spectra of 0.05 mM cytochrome c at different applied potentials in the CNT film OTTLE are shown in Figure 8B. From the spectroelectrochemical Nernst equation (absorbance at 314 nm was used for the calculations), the E°' was determined at 27.0 ± 2.5 mV vs Ag/AgCl which corresponds well with reported values on ITO electrode.³⁷ The n value for cytochrome c was measured as 0.86 ± 0.06 , which is somewhat lower than the expected value of unity. By comparison with direct electron transfer at a gold minigrid electrode, which takes hours,⁷ direct electrolysis of cytochrome c at the CNT film OTE was very fast, taking only a few minutes to reach equilibrium for each applied potential. In conclusion, the excellent transparency and adequate conductivity have made the CNT film a unique material to use as an OTE for thin layer spectroelectrochemistry.

CONCLUSIONS

CNT films synthesized by CVD were aligned on a substrate quartz slide to form CNT film OTEs. Spectroscopic studies of the CNT film showed excellent transparency of this material at 1 and 2 layers, which gave adequate conductivity for thin layer spectroelectrochemistry. Unlike most commonly used metal oxide transparent electrodes, the detectable UV/near UV region was extended down to 200 nm using the transparent CNT film. Electrochemical studies including CV and EIS on CNT film demonstrated that the conductivity of the CNT film was directly proportional to the number of layers of the CNT film, but the overall electrochemical response was still limited by the ohmic drop along the CNT thread. Fast electron transfer was observed for the $\text{Fe}(\text{CN})_6^{3-}/\text{Fe}(\text{CN})_6^{4-}$ redox couple. The potential of using this material as an OTE for thin layer

spectroelectrochemistry was examined with 2 model systems, and good correlations have been obtained with the known properties of tris(2,2'-bipyridine) ruthenium(II) chloride and cytochrome c. In conclusion, the CNT film OTE functioned well for thin layer spectroelectrochemistry and is recommended for the cases where measurements in the UV down to 200 nm are needed and when the special properties of the CNT electrode are advantageous such as for direct electron transfer with a heme protein. Fragility and resistance, especially when handling only a few layers, are issues that can limit its broader application.

ASSOCIATED CONTENT

Supporting Information

The Supporting Information is available free of charge on the ACS Publications website at DOI: [10.1021/acs.analchem.5b01784](https://doi.org/10.1021/acs.analchem.5b01784).

Transmission and absorption spectra; SEM image; comparison of peak currents and peak separation for cyclic voltammograms ([PDF](#))

AUTHOR INFORMATION

Corresponding Author

*Telephone: 01-513-556-9210. Fax: 01-513-556-9239. E-mail: William.Heineman@uc.edu.

Notes

The authors declare no competing financial interest.

ACKNOWLEDGMENTS

The authors acknowledge financial support provided by a University of Cincinnati Research Council-Renewable Energy Grant.

REFERENCES

- (1) Kaim, W.; Fiedler, J. *Chem. Soc. Rev.* **2009**, *38*, 3373–3382.
- (2) Kissinger, P. T.; Heineman, W. R. *Laboratory Techniques in Electroanalytical Chemistry*, 2nd ed.; Marcel Dekker: New York, 1996.
- (3) Conklin, S. D.; Heineman, W. R.; Seliskar, C. J. *Electroanalysis* **2007**, *19*, 523–529.
- (4) Krejcik, M.; Danek, M.; Hartl, F. *J. Electroanal. Chem. Interfacial Electrochem.* **1991**, *317*, 179–187.
- (5) Bond, A. M. *Broadening Electrochemical Horizons*; University Press: Oxford, 2002.
- (6) Wang, T.; Schlueter, K. T.; Riehl, B. L.; Johnson, J. M.; Heineman, W. R. *Anal. Chem.* **2013**, *85*, 9486–9492.
- (7) Heineman, W. R.; Norris, B. J.; Goelz, J. F. *Anal. Chem.* **1975**, *47*, 79–84.
- (8) DeAngelis, T. P.; Hurst, R. W.; Yacynych, A. M.; Mark, H. B., Jr.; Heineman, W. R.; Mattson, J. S. *Anal. Chem.* **1977**, *49*, 1395–1398.
- (9) Zudans, I.; Paddock, J. R.; Kuramitz, H.; Maghasi, A. T.; Wansapura, C. M.; Conklin, S. D.; Kaval, N.; Shtoyko, T.; Monk, D. J.; Bryan, S. A.; Hubler, T. L.; Richardson, J. N.; Seliskar, C. J.; Heineman, W. R. *J. Electroanal. Chem.* **2004**, *565*, 311–320.
- (10) Norvell, V. E.; Mamantov, G. *Anal. Chem.* **1977**, *49*, 1470–1472.
- (11) Dewald, H. D.; Watkins, J. W., II; Elder, R. C.; Heineman, W. R. *Anal. Chem.* **1986**, *58*, 2968–2975.
- (12) Hecht, D. S.; Hu, L.; Irvin, G. *Adv. Mater.* **2011**, *23*, 1482–1513.
- (13) Kumar, A.; Zhou, C. *ACS Nano* **2010**, *4*, 11–14.
- (14) Iijima, S. *Nature* **1991**, *354*, 56–58.
- (15) De Volder, M. F. L.; Tawfick, S. H.; Baughman, R. H.; Hart, A. J. *Science* **2013**, *339*, 535–539.
- (16) Wang, T.; Manamperi, H. D.; Yue, W.; Riehl, B. L.; Riehl, B. D.; Johnson, J. M.; Heineman, W. R. *Electroanalysis* **2013**, *25*, 983–990.
- (17) Wang, T.; Zhao, D.; Guo, X.; Correa, J.; Riehl, B. L.; Heineman, W. R. *Anal. Chem.* **2014**, *86*, 4354–4361.
- (18) Endo, M.; Hayashi, T.; Kim, Y. *Pure Appl. Chem.* **2006**, *78*, 1703–1713.
- (19) Kumar, M.; Ando, Y. *J. Nanosci. Nanotechnol.* **2010**, *10*, 3739–3758.
- (20) Prasek, J.; Drbohlavova, J.; Chomoucka, J.; Hubalek, J.; Jasek, O.; Adam, V.; Kizek, R. *J. Mater. Chem.* **2011**, *21*, 15872–15884.
- (21) Rafique, M. M. A.; Iqbal, J. *J. Encapsulation Adsorpt. Sci.* **2011**, *1*, 29–34.
- (22) Endo, M.; Takeuchi, K.; Igarashi, S.; Kobori, M.; Shiraishi, M.; Kroto, H. W. *19th Meeting Japanese Carbon Society*, Japanese Carbon Society, Kyoto, 1992; p 192.
- (23) Jose-Yacaman, M.; Miki-Yoshida, M.; Rendon, L.; Santiesteban, J. *G. Appl. Phys. Lett.* **1993**, *62*, 657.
- (24) Koziol, K.; Vilatela, J.; Moisala, A.; Motta, M.; Cunniff, P.; Sennett, M.; Windle, A. *Science* **2007**, *318*, 1892–1895.
- (25) Futaba, D. N.; Hata, K.; Yamada, T.; Hiraoka, T.; Hayamizu, Y.; Kakudate, Y.; Tanaike, O.; Hatori, H.; Yumura, M.; Iijima, S. *Nat. Mater.* **2006**, *5*, 987–994.
- (26) Hayamizu, Y.; Yamada, T.; Mizuno, K.; Davis, R. C.; Futaba, D. N.; Yumura, M.; Hata, K. *Nat. Nanotechnol.* **2008**, *3*, 289–294.
- (27) De Volder, M. F. L.; Tawfick, S. H.; Park, S. J.; Copic, D.; Zhao, Z.; Lu, W.; Hart, A. J. *Adv. Mater.* **2010**, *22*, 4384–4389.
- (28) Zhang, M.; Atkinson, K. R.; Baughman, R. H. *Science* **2004**, *306*, 1358–1361.
- (29) Jiang, K.; Li, Q.; Fan, S. *Nature* **2002**, *419*, 801.
- (30) Wu, Z.; Chen, Z.; Du, X.; Logan, J.; Sippel, J.; Nikilou, M.; Kamara, K.; Reynolds, J. R.; Tanner, D. B.; Hebard, A. F.; Rinzler, A. G. *Science* **2004**, *305*, 1273–1276.
- (31) Chen, T.; Peng, H.; Durstock, M.; Dai, L. *Sci. Rep.* **2014**, *4*, 3162–3168.
- (32) Cai, L.; Song, L.; Luan, P.; Zhang, Q.; Zhang, N.; Gao, Q.; Zhao, D.; Zhang, X.; Tu, M.; Yang, F.; Zhou, W.; Fan, Q.; Fan, Q.; Luo, J.; Zhou, W.; Aiayan, P. M.; Xie, S. *Sci. Rep.* **2013**, *3*, 3048–3055.
- (33) Yu, Z.; Niu, X.; Liu, Z.; Pei, Q. *Adv. Mater.* **2011**, *23*, 3989–3994.
- (34) Niu, Z.; Dong, H.; Zhu, B.; Li, J.; Hng, H.; Zhou, W.; Chen, X.; Xie, S. *Adv. Mater.* **2013**, *25*, 1058–1064.
- (35) Sekitani, T.; Nakajima, H.; Maeda, H.; Fukushima, T.; Aida, T.; Hata, K.; Someya, T. *Nat. Mater.* **2009**, *8*, 494–499.
- (36) Xiao, L.; Chen, Z.; Feng, C.; Liu, L.; Bai, Z.; Wang, Y.; Qian, L.; Zhang, Y.; Li, Q.; Jiang, K.; Fan, S. *Nano Lett.* **2008**, *8*, 4539–4545.
- (37) Jung, Y.; Kar, S.; Talapatra, S.; Soldano, C.; Viswanathan, G.; Li, X.; Yao, Z.; Ou, F.; Avadhanula, A.; Vajtai, R.; Curran, S.; Nalamasu, O.; Ajayan, P. M. *Nano Lett.* **2006**, *6*, 413–418.
- (38) Alvarez, N. T.; Miller, P.; Haase, M.; Kienzle, N.; Zhang, L.; Schulz, M.; Shanov, V. *Carbon* **2015**, *86*, 350–357.
- (39) Jayasinghe, C.; Chakrabarti, S.; Schulz, M. J.; Shanov, V. *J. Mater. Res.* **2011**, *26*, 645–651.
- (40) Jiang, K.; Li, Q.; Fan, S. *Nature* **2002**, *419*, 801.
- (41) Wilson, R. A.; Pinyayev, T. S.; Membreño, N.; Heineman, W. R. *Electroanalysis* **2010**, *22*, 2162–2166.
- (42) Costa, S.; Borowiak-Palen, E.; Kruszynska, M.; Bachmatiuk, A.; Kalenczuk, R. *J. Mater. Sci. Poland* **2008**, *26*, 433–440.
- (43) Rance, G. A.; Marsh, D. H.; Nicholas, R. J.; Khlobystov, A. N. *Chem. Phys. Lett.* **2010**, *493*, 19–23.
- (44) Guo, G.; Chu, K.; Wang, D.; Duan, C. *Phys. Rev. B: Condens. Matter Mater. Phys.* **2004**, *69*, 205416.
- (45) Takagi, Y.; Okada, S. *Phys. Rev. B: Condens. Matter Mater. Phys.* **2009**, *79*, 233406.
- (46) Keiser, H.; Beccu, K. D.; Gutjahr, M. A. *Electrochim. Acta* **1976**, *21*, 539–543.
- (47) Pasta, M.; La Mantia, F.; Cui, Y. *Electrochim. Acta* **2010**, *55*, 5561–5568.
- (48) Kalyanasundaram, K. *Coord. Chem. Rev.* **1982**, *46*, 159–244.
- (49) Heineman, W. R. *J. Chem. Educ.* **1983**, *60*, 305–308.
- (50) Wang, L.; Wang, E. *Electrochim. Commun.* **2004**, *6*, 49–54.

- (51) Schaming, D.; Renault, C.; Tucker, R. T.; et al. *Langmuir* **2012**, *28*, 14065–14072.
- (52) Matsuda, N.; Santos, J.; Takatsu, A.; Kato, K. *Thin Solid Films* **2003**, *438-439*, 403–406.
- (53) Shie, J.; Yogeswaran, U.; Chen, S. *Talanta* **2008**, *74*, 1659–1669.
- (54) Zhao, H.; Du, Q.; Li, Z.; Yang, Q. *Sensors* **2012**, *12*, 10450–10462.